WEIZMANN INSTITUTE OF SCIENCE

Primordial Gravitational Waves and Pulsar Timing Array Data

E.M., Morgante, Puchades Ibáñez, Ramberg, Ratzinger, Schenk, and Schwaller

JHEP **10** (2023), 171 [arXiv:2306.14856 [hep-ph]]

Eric Madge

DESY – November 1, 2023

Motivation

NANOGrav, 12.5 year dataset

[NANOGrav (APJL 2020)]

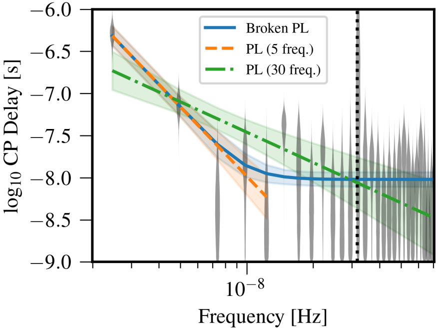

NANOGrav, 15 year dataset

[NANOGrav (APJL 2023)]

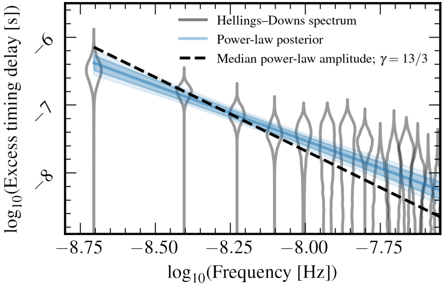

SGWB

astrophysical?

cosmological?

Motivation

NANOGrav, 12.5 year dataset

[NANOGrav (APJL 2020)]

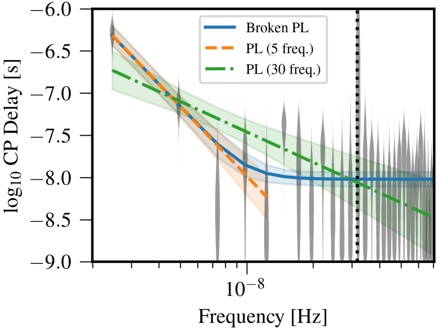

NANOGrav, 15 year dataset

[NANOGrav (APJL 2023)]

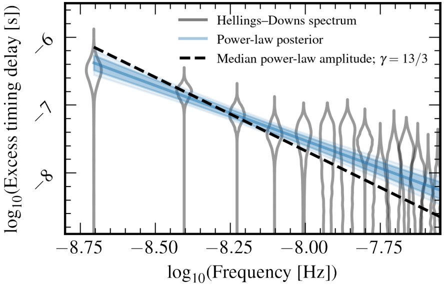

SGWB

astrophysical?

cosmological?

here:
- benchmark models
- cosmological constraints

Outlook

1. Pulsar Timing Arrays
2. Cosmological Phase Transitions
3. Domain Walls
4. Bosonic Instabilities
5. Conclusions

Pulsar Timing Arrays

Pulsar Timing Arrays

- pulsar = rapidly rotating neutron star

  $\Longrightarrow$ cosmic lighthouse

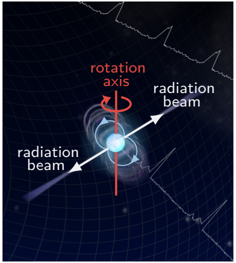

[Credit: T. Klein, NANOGrav; modified]

Pulsar Timing Arrays

- pulsar = rapidly rotating neutron star
  $\Longrightarrow$ cosmic lighthouse

- pulsar timing arrays (PTAs)
  GW detection via correlations in timing residuals $\Longrightarrow$ $f \sim \mathrm{nHz}$

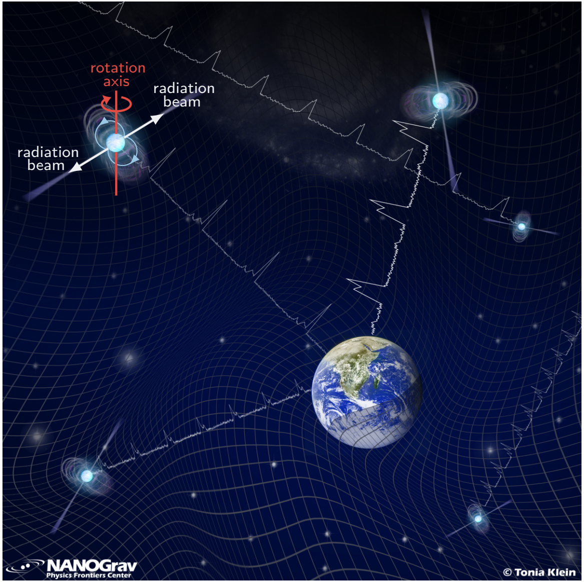

[Credit: T. Klein, NANOGrav; modified]

Pulsar Timing Arrays

- pulsar $=$ rapidly rotating neutron star

  $\Longrightarrow$ cosmic lighthouse

- pulsar timing arrays (PTAs)

  GW detection via correlations in timing residuals $\Longrightarrow$ $f \sim$ nHz

- operating PTAs:

collaboration	N_P	T_obs	ref.
EPTA	25	25 yrs	[A&A 2023]
NANOGrav	67	15 yrs	[APJL 2023]
PPTA	30	18 yrs	[PASA 2023]
InPTA	14	3.5 yrs	[PASA 2022]
CPTA	57	3.5 yrs	[in prep.]
IPTA	65	20 yrs	[MNRAS 2019]

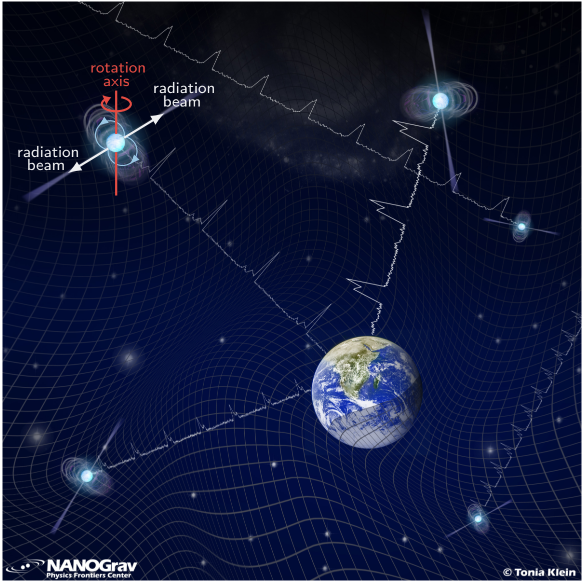

[Credit: T. Klein, NANOGrav; modified]

PTA Signal

- since Sept. 2020:

  strong evidence for common red-noise process

  [NANOGrav (APJL 2020); PPTA (APJL 2021); EPTA (MNRAS 2021); IPTA (MNRAS 2022)]

- since June 28, 2023:

  strong evidence for Hellings-Downs correlations

  [NANOGrav (APJL 2023); EPTA (A&A 2023); PPTA (APJL 2023); CPTA (RAA 2023)]

  $\Longrightarrow$ GW background

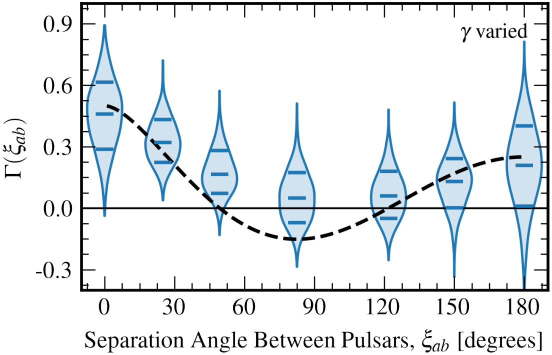

[NANOGrav (APJL 2023)]

PTA Signal

- since Sept. 2020:

  strong evidence for common red-noise process

  [NANOGrav (APJL 2020); PPTA (APJL 2021); EPTA (MNRAS 2021); IPTA (MNRAS 2022)]

- since June 28, 2023:

  strong evidence for Hellings-Downs correlations

  [NANOGrav (APJL 2023); EPTA (A&A 2023); PPTA (APJL 2023); CPTA (RAA 2023)]

  $\Longrightarrow$ GW background

- consistent with expected SGWB from SMBHBs:

$$h_c = A \left(\frac{f}{1\,\mathrm{yr}^{-1}} \right)^{\frac{3-\gamma}{2}} \quad \text{with } \gamma = \frac{13}{3}$$

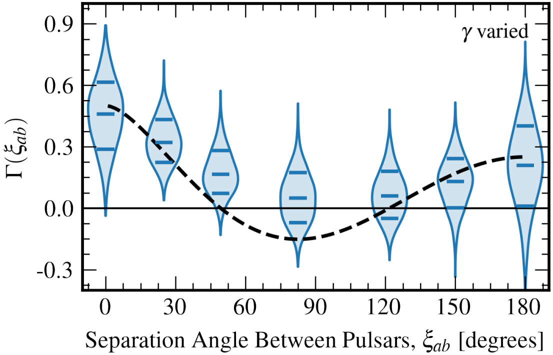

[NANOGrav (APJL 2023)]

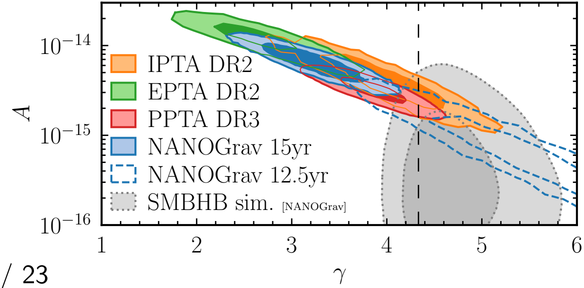

Primordial Sources of SGWBs

phase transitions, cosmic strings, domain walls, bosonic instabilities, inflation, ...

Primordial Sources of SGWBs

phase transitions, cosmic strings, domain walls, bosonic instabilities, inflation, ...

- frequency: $$f_0 \sim \frac{a_0}{a_*} H_* \underbrace{\frac{f_*}{H_*}}_{\lesssim 1} \sim 1\,\mathrm{nHz}\,\frac{T_*}{10\,\mathrm{MeV}}\,\frac{f_*}{H_*}$$

Primordial Sources of SGWBs

phase transitions, cosmic strings, domain walls, bosonic instabilities, inflation, ...

- frequency: $$f_0 \sim \frac{a_0}{a_*} H_* \underbrace{\frac{f_*}{H_*}}_{\lesssim 1} \sim 1\,\text{nHz}\,\frac{T_*}{10\,\text{MeV}}\,\frac{f_*}{H_*}$$

- amplitude: $$\rho_{\text{GW}} \sim M_{\text{pl}}^2 \langle \dot{h}_{ij} \dot{h}_{ij} \rangle, \qquad \Box \bar{h}_{\mu\nu} \sim \frac{T_{\mu\nu}}{M_{\text{pl}}^2}$$

$$\Longrightarrow \quad \Omega_{\text{GW}} \sim \left(\frac{a_*}{a_0}\right)^4 \frac{1}{\rho_c} \frac{\rho_{\text{source}}^2}{f_*^2 M_{\text{pl}}^2} \sim \left(\frac{a_*}{a_0}\right)^4 \left(\frac{H_0}{H_*}\right)^2 \left(\frac{H_*}{f_*}\right)^2 \Omega_{\text{source}}^2$$

Primordial Sources of SGWBs

phase transitions, cosmic strings, domain walls, bosonic instabilities, inflation, ...

- frequency: $$f_0 \sim \frac{a_0}{a_*} H_* \underbrace{\frac{f_*}{H_*}}_{\lesssim 1} \sim 1\,\text{nHz}\, \frac{T_*}{10\,\text{MeV}}\, \frac{f_*}{H_*}$$

- amplitude: $$\rho_{\text{GW}} \sim M_{\text{pl}}^2 \langle \dot{h}_{ij} \dot{h}_{ij} \rangle, \qquad \Box \bar{h}_{\mu\nu} \sim \frac{T_{\mu\nu}}{M_{\text{pl}}^2}$$

$$\Longrightarrow \quad \Omega_{\text{GW}} \sim \left(\frac{a_*}{a_0}\right)^4 \frac{1}{\rho_c} \frac{\rho_{\text{source}}^2}{f_*^2 M_{\text{pl}}^2} \sim \left(\frac{a_*}{a_0}\right)^4 \left(\frac{H_0}{H_*}\right)^2 \left(\frac{H_*}{f_*}\right)^2 \Omega_{\text{source}}^2$$

$\Longrightarrow$ for PTAs: $T_* \sim \text{few MeV}, \qquad \Omega_{\text{source}} \gtrsim 0.1$

Cosmological Phase Transitions

Cosmological Phase Transitions

- thermal corrections typically restore spontaneously broken symmetries at high temperatures
  $\implies$ symmetry breaking phase transition
- can be crossover or first-order

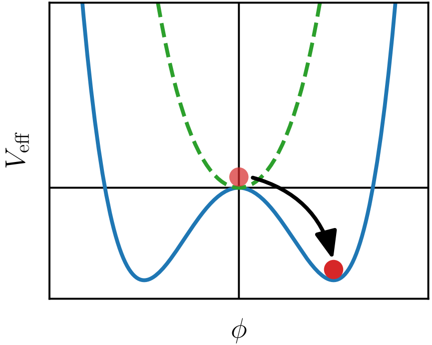

Cosmological Phase Transitions

- thermal corrections typically restore spontaneously broken symmetries at high temperatures
  $\Longrightarrow$ symmetry breaking phase transition
- can be crossover or first-order

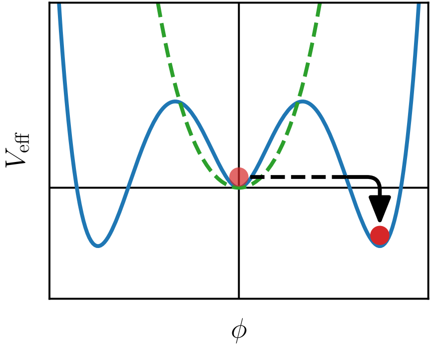

Cosmological Phase Transitions

- thermal corrections typically restore spontaneously broken symmetries at high temperatures
  $\Longrightarrow$ symmetry breaking phase transition
- can be crossover or first-order

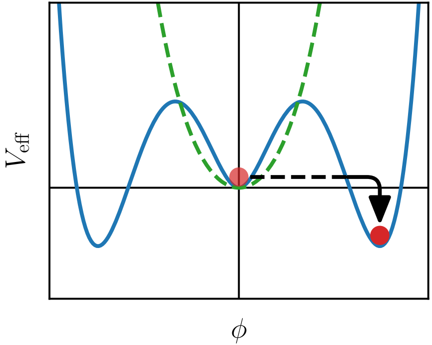

GW production:

1. vacuum bubble collisions

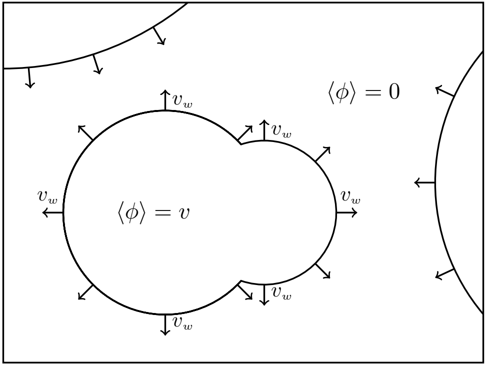

Cosmological Phase Transitions

- thermal corrections typically restore spontaneously broken symmetries at high temperatures
  $\Longrightarrow$ symmetry breaking phase transition
- can be crossover or first-order

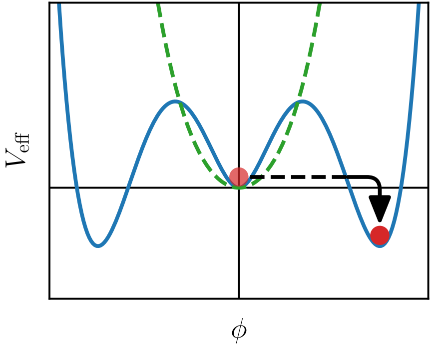

GW production:

1. vacuum bubble collisions
2. sound waves collisions

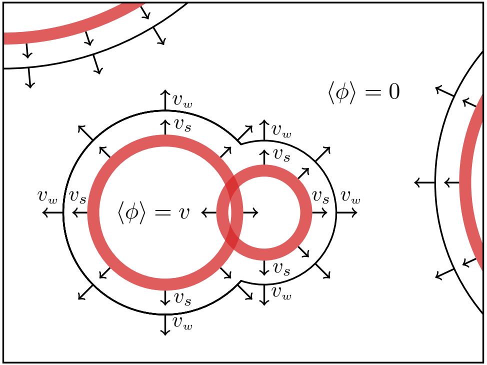

Cosmological Phase Transitions

- thermal corrections typically restore spontaneously broken symmetries at high temperatures
  $\Longrightarrow$ symmetry breaking phase transition
- can be crossover or first-order

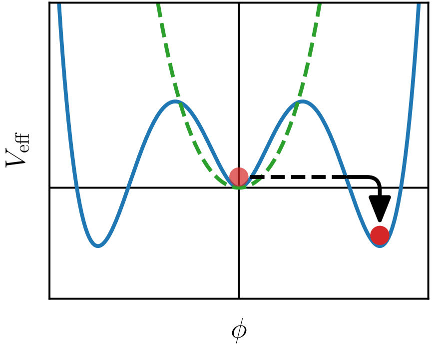

GW production:

1. vacuum bubble collisions
2. sound waves collisions
3. turbulence and vortical motion

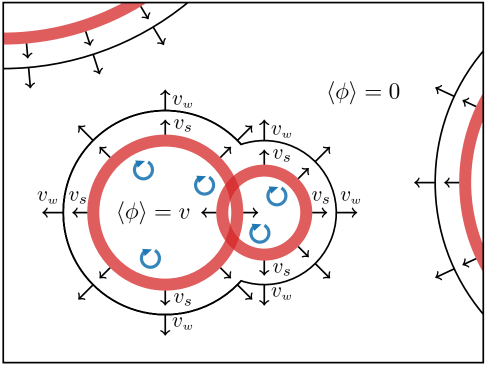

Gravitational Wave Spectrum

- peak frequency:

$$f_p \propto T_* \frac{1}{R_* H_*} \sim 10\,\text{nHz}\,\frac{T_*}{10\,\text{MeV}}\,\frac{\beta/H_*}{10}$$

$$\alpha \approx \frac{\Delta V}{\rho_R}, \quad \beta = \frac{\dot{\Gamma}}{\Gamma} \approx \frac{3}{R_*}$$

Gravitational Wave Spectrum

- peak frequency:

$$f_p \propto T_* \frac{1}{R_* H_*} \sim 10\,\text{nHz}\,\frac{T_*}{10\,\text{MeV}}\,\frac{\beta/H_*}{10}$$

- peak amplitude: (for collisions)

$$h^2\Omega_p \propto \left(\frac{\Delta V}{\Delta V + \rho_R}\right)^2 (R_* H_*)^2 \sim 10^{-8} \left(\frac{10}{\beta/H_*}\right)^2 \left(\frac{\alpha}{1+\alpha}\right)^2$$

$$\alpha \approx \frac{\Delta V}{\rho_R}, \quad \beta = \frac{\dot{\Gamma}}{\Gamma} \approx \frac{3}{R_*}$$

Gravitational Wave Spectrum

- peak frequency:

$$f_p \propto T_* \frac{1}{R_* H_*} \sim 10\,\text{nHz}\, \frac{T_*}{10\,\text{MeV}} \frac{\beta/H_*}{10}$$

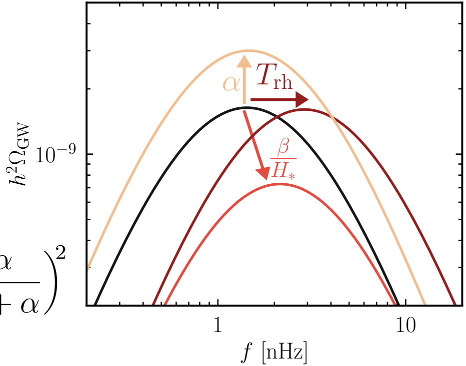

- peak amplitude: (for collisions)

$$h^2\Omega_p \propto \left(\frac{\Delta V}{\Delta V + \rho_R}\right)^2 (R_* H_*)^2 \sim 10^{-8} \left(\frac{10}{\beta/H_*}\right)^2 \left(\frac{\alpha}{1+\alpha}\right)^2$$

- spectral shape: [from Lewicki, Vaskonen (EPJC 2023)]

$$\Omega_{\rm GW} = \Omega_p \frac{(a+b)^c}{\left[b\,(f/f_p)^{-a/c} + a\,(f/f_p)^{b/c}\right]^c}\,, \qquad a = 2.41,\; b = 2.42,\; c = 4.08$$

$$\alpha \approx \frac{\Delta V}{\rho_R}, \qquad \beta = \frac{\dot\Gamma}{\Gamma} \approx \frac{3}{R_*}$$

Gravitational Wave Spectrum

- peak frequency:

$$f_p \propto T_* \frac{1}{R_* H_*} \sim 10\,\text{nHz}\,\frac{T_*}{10\,\text{MeV}}\,\frac{\beta/H_*}{10}$$

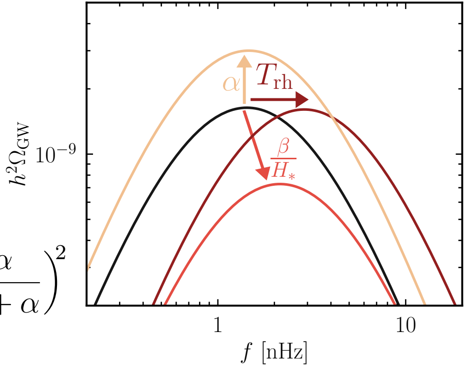

- peak amplitude: (for collisions)

$$h^2\Omega_p \propto \left(\frac{\Delta V}{\Delta V + \rho_R}\right)^2 (R_* H_*)^2 \sim 10^{-8}\left(\frac{10}{\beta/H_*}\right)^2 \left(\frac{\alpha}{1+\alpha}\right)^2$$

- spectral shape: [from Lewicki, Vaskonen (EPJC 2023)]

$$\Omega_{\rm GW} = \Omega_p \frac{(a+b)^c}{\left[b\,(f/f_p)^{-a/c} + a\,(f/f_p)^{b/c}\right]^c}\,, \qquad a = 2.41,\ b = 2.42,\ c = 4.08$$

- for PTAs: $h^2\Omega \sim 10^{-9} \implies \alpha \gtrsim 1$

$$\alpha \approx \frac{\Delta V}{\rho_R}, \quad \beta = \frac{\dot\Gamma}{\Gamma} \approx \frac{3}{R_*}$$

Gravitational Wave Spectrum

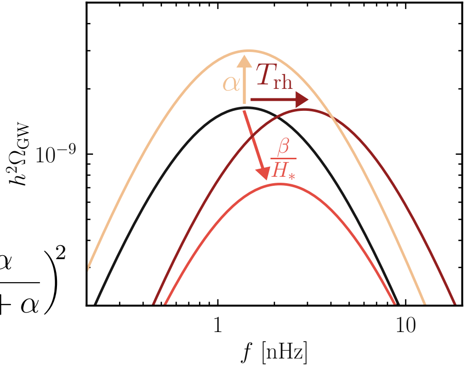

- peak frequency:

$$f_p \propto T_{\rm rh} \frac{1}{R_* H_*} \sim 10\,\text{nHz}\, \frac{T_{\rm rh}}{10\,\text{MeV}} \frac{\beta/H_*}{10}$$

- peak amplitude: (for collisions)

$$h^2\Omega_p \propto \left(\frac{\Delta V}{\Delta V + \rho_R}\right)^2 (R_* H_*)^2 \sim 10^{-8} \left(\frac{10}{\beta/H_*}\right)^2 \left(\frac{\alpha}{1+\alpha}\right)^2$$

- spectral shape: [from Lewicki, Vaskonen (EPJC 2023)]

$$\Omega_{\rm GW} = \Omega_p \frac{(a+b)^c}{\left[b\,(f/f_p)^{-a/c} + a\,(f/f_p)^{b/c}\right]^c}\,, \qquad a = 2.41,\; b = 2.42,\; c = 4.08$$

- for PTAs: $h^2\Omega \sim 10^{-9} \quad \Longrightarrow \quad \alpha \gtrsim 1$

$\Longrightarrow$ supercooled PTs $\Longrightarrow$ nearly conformal models

$$\alpha \approx \frac{\Delta V}{\rho_R}, \quad \beta = \frac{\dot\Gamma}{\Gamma} \approx \frac{3}{R_*}$$

Coleman-Weinberg Model

- classically scale-invariant gauged U(1) model [Coleman, Weinberg (PRD '73)]

$$\mathcal{L} \supset -\frac{1}{4}F_{\mu\nu}F^{\mu\nu} + D_\mu\phi^\dagger D^\mu\phi - \frac{\lambda}{4}\left(\phi^\dagger\phi\right)^2$$

- 3 parameters: $g, \ \lambda, \ M$

$$M = \frac{\mu_R}{4\pi}e^{\gamma_E - \frac{1}{3}}$$

Coleman-Weinberg Model

- classically scale-invariant gauged U(1) model [Coleman, Weinberg (PRD '73)]

$$\mathcal{L} \supset -\frac{1}{4} F_{\mu\nu} F^{\mu\nu} + D_\mu \phi^\dagger D^\mu \phi - \frac{\lambda}{4} \left(\phi^\dagger \phi\right)^2$$

- 3 parameters: $g, \cancel{\lambda}, M$

$$M = \frac{\mu_R}{4\pi} e^{\gamma_E - \frac{1}{3}}$$

- for strong PhT: $\lambda \ll g^4$

  (loop-induced SSB $\rightarrow$ need flat direction)

Coleman-Weinberg Model

- classically scale-invariant gauged U(1) model [Coleman, Weinberg (PRD '73)]

$$\mathcal{L} \supset -\frac{1}{4}F_{\mu\nu}F^{\mu\nu} + D_\mu\phi^\dagger D^\mu\phi - \frac{\lambda}{4}\left(\phi^\dagger\phi\right)^2$$

- 3 parameters: $g, \cancel{\lambda}, M$

  $$M = \frac{\mu_R}{4\pi}e^{\gamma_E - \frac{1}{3}}$$

- for strong PhT: $\lambda \ll g^4$
  (loop-induced SSB $\rightarrow$ need flat direction)

- $m_\phi \propto g^2\langle\phi\rangle \propto gM \sim (1 - 100)$ MeV
  $m_A \propto g\langle\phi\rangle \propto M$

Coleman-Weinberg Model

- classically scale-invariant gauged U(1) model [Coleman, Weinberg (PRD '73)]

$$\mathcal{L} \supset -\frac{1}{4} F_{\mu\nu} F^{\mu\nu} + D_\mu \phi^\dagger D^\mu \phi - \frac{\lambda}{4} \left(\phi^\dagger \phi\right)^2$$

- 3 parameters: $g, \cancel{\lambda}, M$

$$M = \frac{\mu_R}{4\pi} e^{\gamma_E - \frac{1}{3}}$$

- for strong PhT: $\lambda \ll g^4$
  (loop-induced SSB $\to$ need flat direction)

- $m_\phi \propto g^2 \langle \phi \rangle \propto gM \sim (1 - 100)$ MeV
  $m_A \propto g \langle \phi \rangle \propto M$

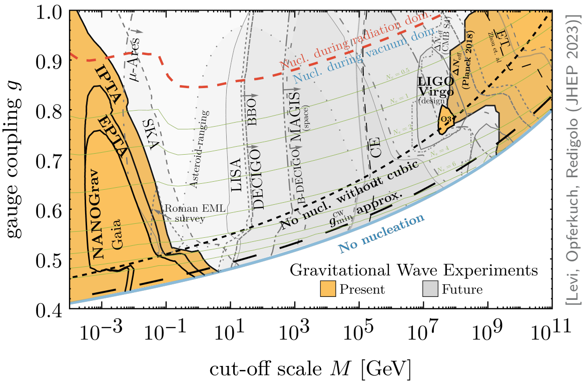

[Levi, Opferkuch, Redigolo (JHEP 2023)]

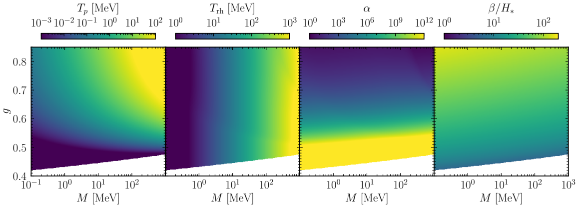

PTA fit - PhT in CW Model

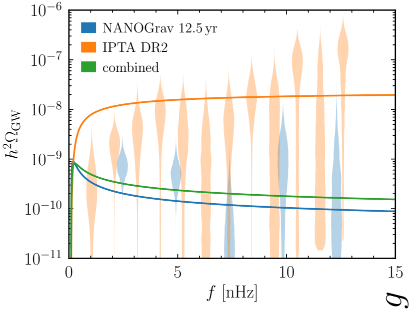

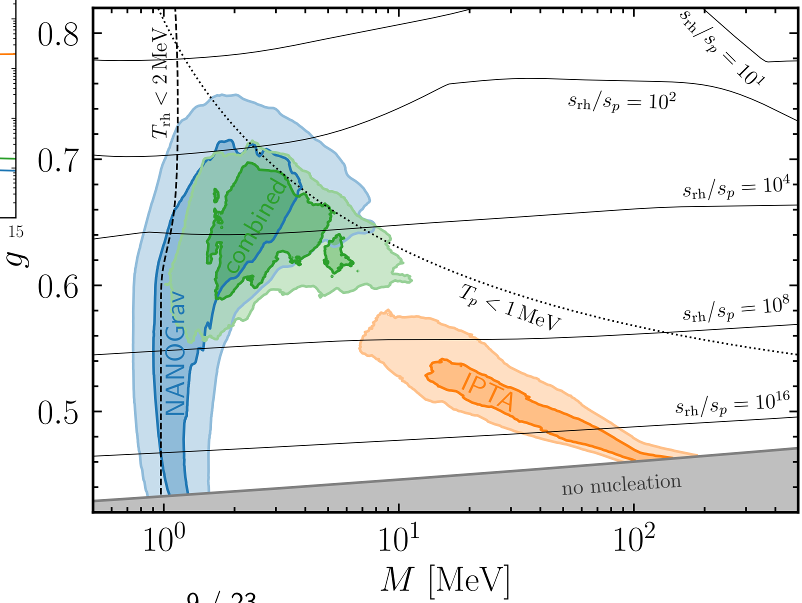

PTA fit - PhT in CW Model

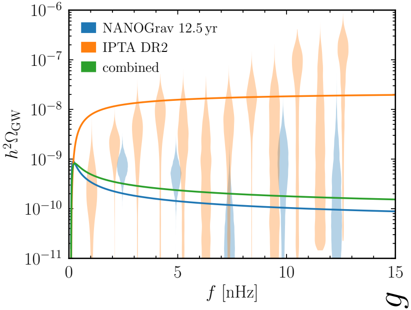

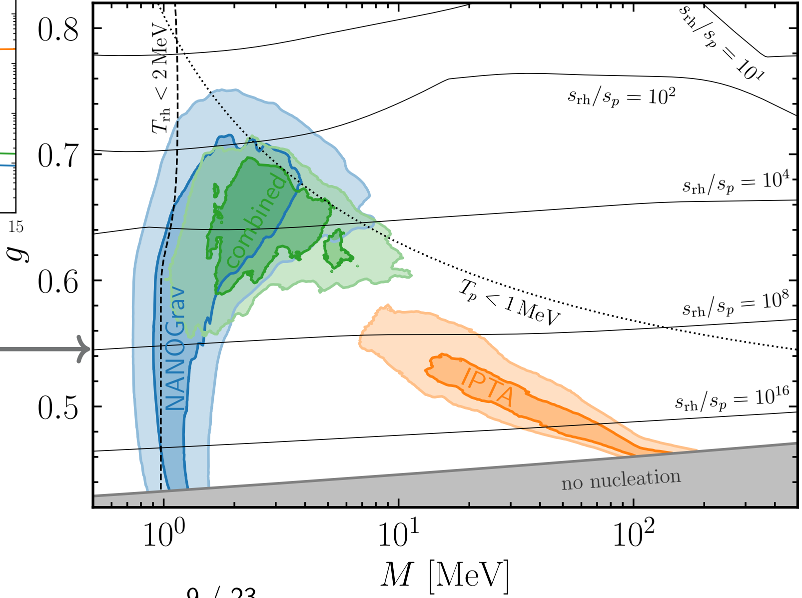

BAU: $\mathcal{O}(1)$ baryon asym. required before reheating (if $\frac{s_{\rm rh}}{s_p} \sim 10^{10}$)

PTA fit - PhT in CW Model

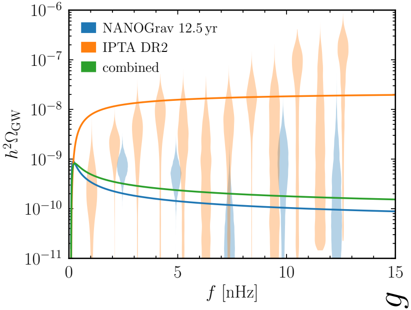

PhT happens after onset of BBN

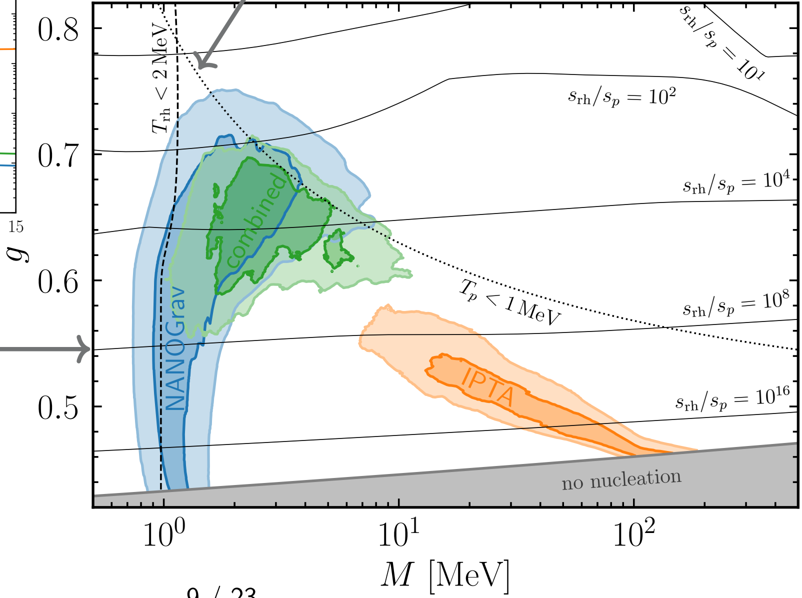

BAU: $\mathcal{O}(1)$ baryon asym. required before reheating (if $\frac{s_{\rm rh}}{s_p} \sim 10^{10}$)

PTA fit - PhT in CW Model

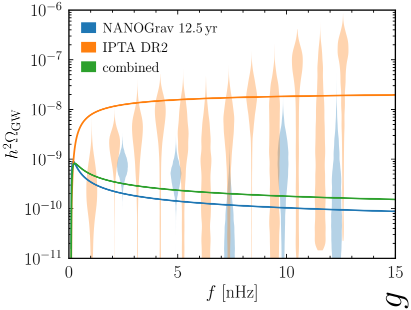

PhT happens after onset of BBN

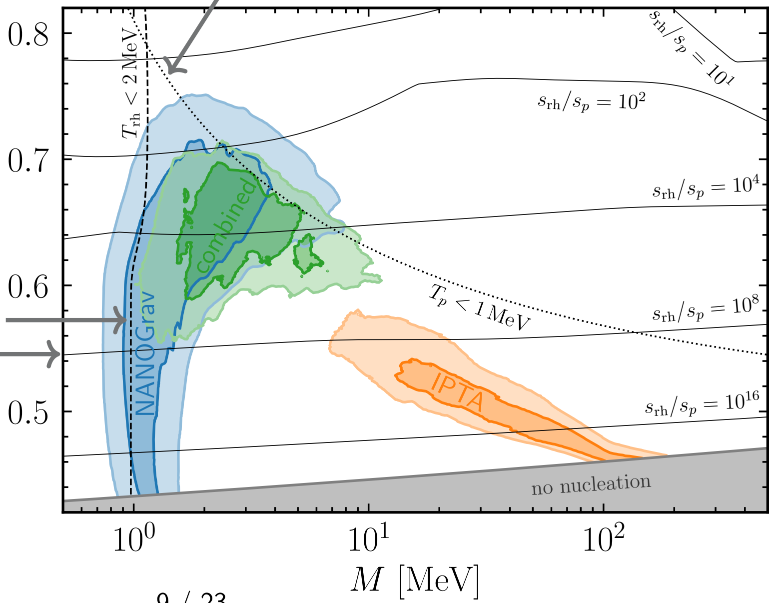

ν-rethermalization

BAU: $\mathcal{O}(1)$ baryon asym. required before reheating (if $\frac{s_{\rm rh}}{s_p} \sim 10^{10}$)

Reheating

- reheating: $\Delta V \longrightarrow \rho_R \quad \Longrightarrow \quad$ requires $\quad \Gamma_\phi \gtrsim H_{\mathsf{rh}} \sim \dfrac{T_{\mathsf{rh}}^2}{M_{\mathsf{pl}}} \gtrsim 4 \times 10^{-20}$ MeV

Reheating

- reheating: $\Delta V \longrightarrow \rho_R \quad \Longrightarrow \quad$ requires $\quad \Gamma_\phi \gtrsim H_{\rm rh} \sim \dfrac{T_{\rm rh}^2}{M_{\rm pl}} \gtrsim 4 \times 10^{-20}$ MeV

- Higgs portal: $\quad \mathcal{L} \supset \lambda_p \, |\phi|^2 \, |H|^2 \quad \longrightarrow \quad$ mixing
  - $\lambda_p \sim 10^{-4} \quad \Longrightarrow \quad \Delta m_\phi^2 \sim \lambda_p v_H^2 \sim \mathrm{GeV}^2$

Reheating

- reheating: $\Delta V \longrightarrow \rho_R \quad \Longrightarrow \quad$ requires $\quad \Gamma_\phi \gtrsim H_{\text{rh}} \sim \dfrac{T_{\text{rh}}^2}{M_{\text{pl}}} \gtrsim 4 \times 10^{-20}$ MeV

- Higgs portal: $\quad \mathcal{L} \supset \cancel{\lambda_p |\phi|^2 |H|^2} \quad \longrightarrow \quad$ mixing
  - $\lambda_p \sim 10^{-4} \quad \Longrightarrow \quad \Delta m_\phi^2 \sim \lambda_p v_H^2 \sim \text{GeV}^2$
  - violates scale invariance

Reheating

- reheating: $\Delta V \longrightarrow \rho_R \quad \Longrightarrow \quad$ requires $\quad \Gamma_\phi \gtrsim H_{\text{rh}} \sim \dfrac{T_{\text{rh}}^2}{M_{\text{pl}}} \gtrsim 4 \times 10^{-20}$ MeV

- Higgs portal: $\quad \mathcal{L} \supset \cancel{\lambda_p |\phi|^2 |H|^2} \quad \longrightarrow \quad$ mixing
  - $\lambda_p \sim 10^{-4} \quad \Longrightarrow \quad \Delta m_\phi^2 \sim \lambda_p v_H^2 \sim \text{GeV}^2$
  - violates scale invariance

- direct coupling to e, γ: $\quad \mathcal{L} \supset c_e \dfrac{|\phi|^2}{\Lambda^2} L H \bar{e} + c_\gamma \dfrac{|\phi|^2}{\Lambda^2} F_{\mu\nu} F^{\mu\nu} \qquad$ ✓
  - does not violate scale invariance
  - $\phi \to e^+ e^-, \ \gamma\gamma$ searches e.g. at MESA

Domain Walls

Domain Walls

- from spontaneously broken discrete symmetry (e.g. Z_2) after inflation

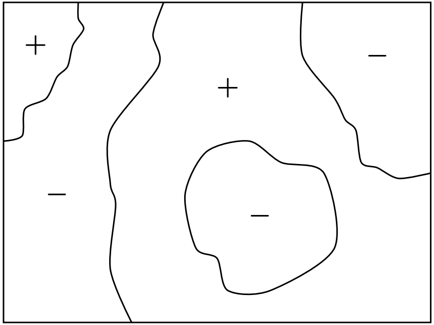

- DWs stretched to horizon size if friction negligible

  $\Longrightarrow$ scaling regime: $\sim$ 1 DW/Hubble

$$\rho_{\mathrm{DW}} \propto \frac{\sigma R^2}{R^3} \sim \sigma H$$

- DW domination: $\Omega_{\mathrm{DW}} = \dfrac{\rho_{\mathrm{DW}}}{3M_{\mathrm{pl}}^2 H^2} \sim \dfrac{\sigma}{M_{\mathrm{pl}} T^2} \quad \Longrightarrow \quad T_{\mathrm{dom}} \sim \sqrt{\dfrac{\sigma}{M_{\mathrm{pl}}}}$

Domain Walls

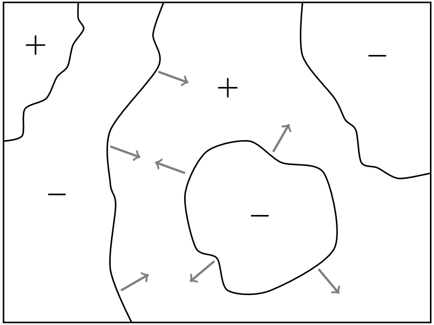

- from spontaneously broken discrete symmetry (e.g. Z_2) after inflation
- DWs stretched to horizon size if friction negligible

  $\Longrightarrow$ scaling regime: $\sim$ 1 DW/Hubble

$$\rho_{\text{DW}} \propto \frac{\sigma R^2}{R^3} \sim \sigma H$$

- DW domination: $\Omega_{\text{DW}} = \dfrac{\rho_{\text{DW}}}{3M_{\text{pl}}^2 H^2} \sim \dfrac{\sigma}{M_{\text{pl}} T^2} \quad \Longrightarrow \quad T_{\text{dom}} \sim \sqrt{\dfrac{\sigma}{M_{\text{pl}}}}$
- need to decay $\Longrightarrow$ add bias V_b

  $\Longrightarrow$ DWs annihilate when $V_b \sim \frac{\sigma}{R}$ $\quad \Longrightarrow \quad T_{\text{ann}} \sim 20\ \text{MeV} \sqrt{\dfrac{\text{TeV}^3}{\sigma} \dfrac{V_b}{\text{MeV}^4}}$

Domain Walls

- from spontaneously broken discrete symmetry (e.g. Z_2) after inflation
- DWs stretched to horizon size if friction negligible

  $\Longrightarrow$ scaling regime: ~ 1 DW/Hubble

$$\rho_{\text{DW}} \propto \frac{\sigma R^2}{R^3} \sim \sigma H$$

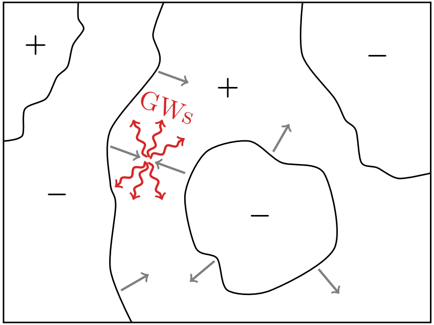

- DW domination: $\Omega_{\text{DW}} = \dfrac{\rho_{\text{DW}}}{3M_{\text{pl}}^2 H^2} \sim \dfrac{\sigma}{M_{\text{pl}} T^2} \quad \Longrightarrow \quad T_{\text{dom}} \sim \sqrt{\dfrac{\sigma}{M_{\text{pl}}}}$
- need to decay $\Longrightarrow$ add bias V_b

  $\Longrightarrow$ DWs annihilate when $V_b \sim \frac{\sigma}{R}$ $\quad \Longrightarrow \quad T_{\text{ann}} \sim 20\,\text{MeV}\sqrt{\dfrac{\text{TeV}^3}{\sigma}\,\dfrac{V_b}{\text{MeV}^4}}$
- GWs dominantly produced in DW collisions around T_{ann}

Gravitational Wave Spectrum

GW production at T_{ann}

- peak frequency:

$$f_p \sim \frac{a}{a_0}\frac{1}{R} \sim 1\,\text{nHz}\,\frac{T_{\text{ann}}}{10\,\text{MeV}}$$

Gravitational Wave Spectrum

GW production at T_{ann}

- peak frequency:

$$f_p \sim \frac{a}{a_0}\frac{1}{R} \sim 1\,\text{nHz}\,\frac{T_{\text{ann}}}{10\,\text{MeV}}$$

- peak amplitude:

$$h^2\Omega_p \sim \left(\frac{a}{a_0}\right)^4 \frac{(\rho_{\text{DW}}R)^2}{\rho_c M_{\text{pl}}^2} \sim 10^{-18}\left(\frac{\sigma}{\text{TeV}^3}\right)^2\left(\frac{T_{\text{ann}}}{10\,\text{MeV}}\right)^{-4}$$

Gravitational Wave Spectrum

GW production at T_{ann}

- peak frequency:

$$f_p \sim \frac{a}{a_0}\frac{1}{R} \sim 1\,\text{nHz}\,\frac{T_{\text{ann}}}{10\,\text{MeV}}$$

- peak amplitude:

$$h^2\Omega_p \sim \left(\frac{a}{a_0}\right)^4 \frac{(\rho_{\text{DW}}R)^2}{\rho_c M_{\text{pl}}^2} \sim 10^{-18}\left(\frac{\sigma}{\text{TeV}^3}\right)^2\left(\frac{T_{\text{ann}}}{10\,\text{MeV}}\right)^{-4}$$

- spectral shape: $$\Omega_{\text{GW}} = \Omega_p \frac{4}{(f/f_p)^{-3} + 3\,(f/f_p)}$$

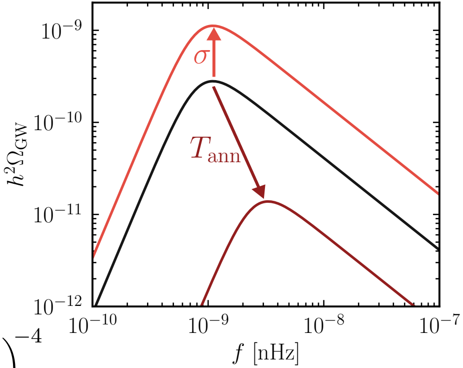

[Ferreira et al. (JCAP 2023)]
[Hitamatsu et al. (JCAP 2014)]

Gravitational Wave Spectrum

GW production at T_{ann}

- peak frequency:

$$f_p \sim \frac{a}{a_0}\,\frac{1}{R} \sim 1\,\text{nHz}\,\frac{T_{\text{ann}}}{10\,\text{MeV}}$$

- peak amplitude:

$$h^2\Omega_p \sim \left(\frac{a}{a_0}\right)^4 \frac{(\rho_{\text{DW}}R)^2}{\rho_c M_{\text{pl}}^2} \sim 10^{-18}\left(\frac{\sigma}{\text{TeV}^3}\right)^2\left(\frac{T_{\text{ann}}}{10\,\text{MeV}}\right)^{-4}$$

- spectral shape:

$$\Omega_{\text{GW}} = \Omega_p\,\frac{4}{(f/f_p)^{-3} + 3\,(f/f_p)}$$

- for PTAs: $T_{\text{ann}} \sim$ few MeV, $\quad h^2\Omega_{\text{DW}} \sim 0.1$

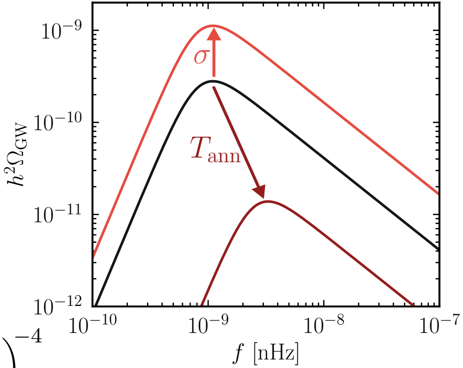

[Ferreira et al. (JCAP 2023)]
[Hitamatsu et al. (JCAP 2014)]

ALP Domain Walls

$$\mathcal{L} \supset \quad \partial_\mu \phi^\dagger \partial^\mu \phi \quad - \underbrace{\lambda \left(\phi^\dagger \phi - \frac{v^2}{2}\right)^2}_{\substack{\text{breaks U(1) spontaneously} \\ \text{w/ } \phi = \frac{v+\rho}{\sqrt{2}}\, e^{i\frac{a}{v}}}} \quad - \underbrace{m_a^2 f_a^2 \left[1 - \cos\frac{a}{f_a}\right]}_{\substack{\text{explicit breaking} \\ \text{U(1)} \to Z_N \\ \text{w/ } f_a = v/N \\ \Rightarrow \text{ DW stable if } N \geq 2}}$$

ALP Domain Walls

$$\mathcal{L} \supset \quad \partial_\mu \phi^\dagger \partial^\mu \phi \quad - \underbrace{\lambda \left(\phi^\dagger \phi - \frac{v^2}{2} \right)^2}_{\substack{\text{breaks U(1) spontaneously} \\ \text{w/ } \phi = \frac{v+\rho}{\sqrt{2}} e^{i\frac{a}{v}}}} \quad - \underbrace{m_a^2 f_a^2 \left[1 - \cos \frac{a}{f_a} \right]}_{\substack{\text{explicit breaking} \\ \text{U(1)} \to Z_N \\ \text{w/ } f_a = v/N \\ \Rightarrow \text{DW stable if } N \geq 2}}$$

- **wall tension:** $\sigma = 8 \frac{m_a^{\cancel{2}} f_a^2}{\cancel{m_a}}$ } size of potential barriers / } wall thickness $\sim \lambda_{\text{Coulomb}} \sim m_a^{-1}$

ALP Domain Walls

$$\mathcal{L} \supset \quad \partial_\mu \phi^\dagger \partial^\mu \phi \quad - \underbrace{\lambda \left(\phi^\dagger \phi - \frac{v^2}{2}\right)^2}_{\substack{\text{breaks U(1) spontaneously} \\ \text{w/ } \phi = \frac{v+\rho}{\sqrt{2}} e^{i\frac{a}{v}}}} \quad - \underbrace{m_a^2 f_a^2 \left[1 - \cos\frac{a}{f_a}\right]}_{\substack{\text{explicit breaking} \\ \text{U(1)} \to Z_N \\ \text{w/ } f_a = v/N \\ \Rightarrow \text{DW stable if } N \geq 2}}$$

- wall tension: $\sigma = 8\,\frac{m_a^{\cancel{2}}\, f_a^2}{\cancel{m_a}}$ } size of potential barriers; } wall thickness $\sim \lambda_{\text{Coulomb}} \sim m_a^{-1}$
- additional breaking of Z_N $\Longrightarrow$ V_b

ALP Domain Walls

$$\mathcal{L} \supset \quad \partial_\mu \phi^\dagger \partial^\mu \phi \quad - \underbrace{\lambda \left(\phi^\dagger \phi - \frac{v^2}{2} \right)^2}_{\substack{\text{breaks U(1) spontaneously} \\ \text{w/ } \phi = \frac{v+\rho}{\sqrt{2}} e^{i\frac{a}{v}}}} \quad - \underbrace{m_a^2 f_a^2 \left[1 - \cos \frac{a}{f_a} \right]}_{\substack{\text{explicit breaking} \\ \text{U}(1) \to Z_N \\ \text{w/ } f_a = v/N \\ \Rightarrow \text{ DW stable if } N \geq 2}}$$

- wall tension: $\sigma = 8 \frac{\cancel{m_a^2} f_a^2}{\cancel{m_a}}$ } size of potential barriers } wall thickness $\sim \lambda_{\text{Coulomb}} \sim m_a^{-1}$
- additional breaking of $Z_N \implies V_b$
- DWs annihilate $\longrightarrow$ ALPs $\longrightarrow$ dark radiation $\quad \Delta N_{\text{eff}} \sim \frac{\rho_{\text{DW}}}{T_{\text{ann}}^4} \sim \frac{m_a f_a^2}{M_{\text{pl}} T_{\text{ann}}^2}$

PTA Fit – ALP DWs

[see also Ferreira et al. (JCAP 2023)]

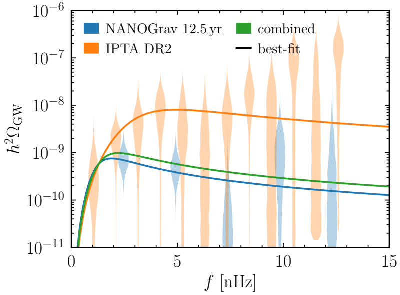

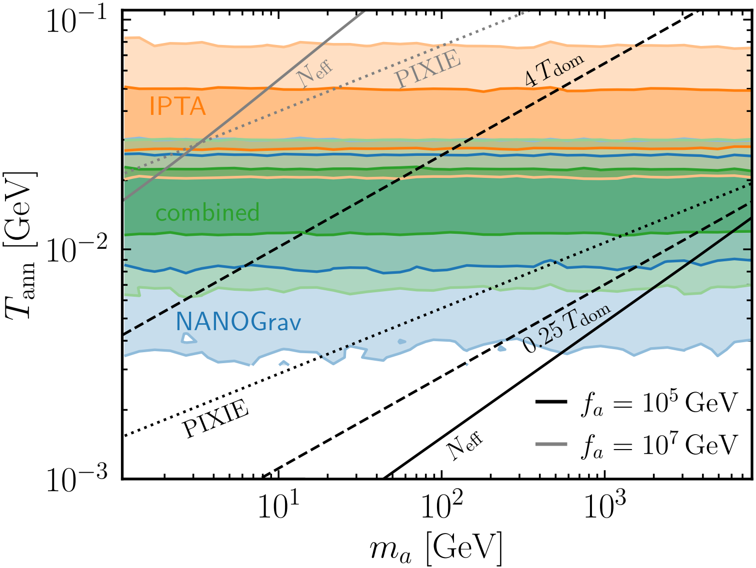

PTA Fit – ALP DWs

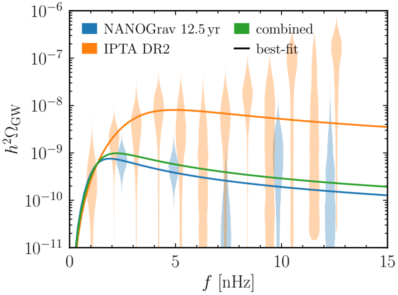

[see also Ferreira et al. (JCAP 2023)]

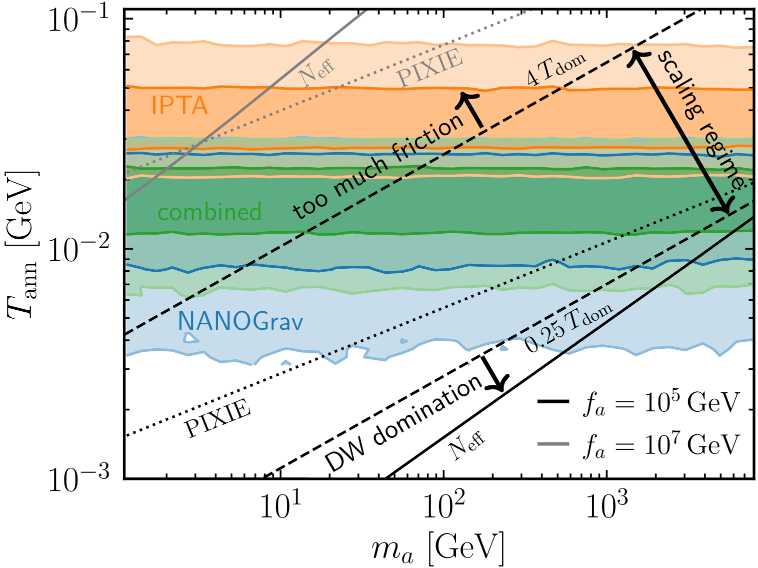

PTA Fit – ALP DWs

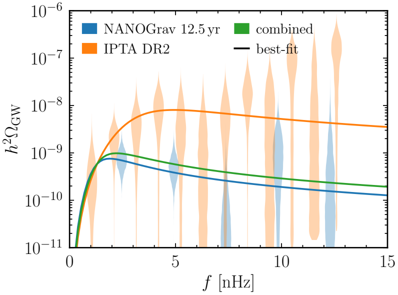

[see also Ferreira et al. (JCAP 2023)]

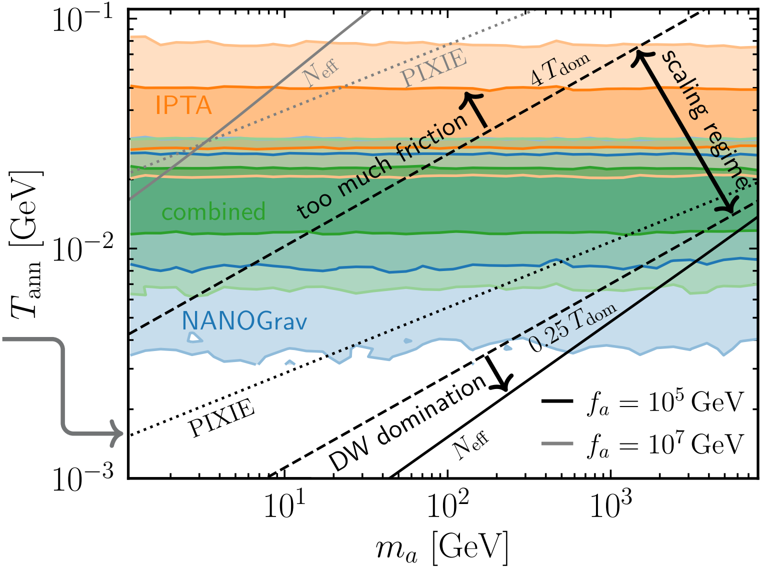

μ-distortions in CMB
[Ramberg, Ratzinger, Schwaller (JCAP 2023)]
from acoustic waves in baryon-photon fluid induced via gravity

Aligned Axion

[Higaki et al. (JHEP 2016)]

- N axions: $$V = \underbrace{\sum_{i=1}^{N} \lambda_i \left(\Phi_i^\dagger \Phi_i - \frac{f_i}{2}\right)^2}_{\text{breaks } \mathrm{U}(1)^N \text{ spontaneously}} + \underbrace{\left[\sum_{i=1}^{N-1} \epsilon_i \Phi_i \Phi_{i+1}^3 + \text{h.c.}\right]}_{\mathrm{U}(1)^{N-1} \text{ explicitly broken to discrete sym.}}$$

Aligned Axion

[Higaki et al. (JHEP 2016)]

- N axions: $$V = \underbrace{\sum_{i=1}^{N} \lambda_i \left(\Phi_i^\dagger \Phi_i - \frac{f_i}{2} \right)^2}_{\text{breaks } \mathrm{U}(1)^N \text{ spontaneously}} + \underbrace{\left[\sum_{i=1}^{N-1} \epsilon_i \Phi_i \Phi_{i+1}^3 + \text{h.c.} \right]}_{\mathrm{U}(1)^{N-1} \text{ explicitly broken to discrete sym.}}$$

  $\Longrightarrow$ $(N-1)$ heavy axions + massless QCD axion

  $\hookrightarrow$ DWs

  $\hookrightarrow$ anomalous $\Longrightarrow V_b \sim \Lambda_{\text{QCD}}^4$

- effective decay constant for QCD axion: $f_{\text{eff}} \sim \sqrt{N}\, 3^N f \gg f$

Aligned Axion

[Higaki et al. (JHEP 2016)]

- N axions: $$V = \underbrace{\sum_{i=1}^{N} \lambda_i \left(\Phi_i^\dagger \Phi_i - \frac{f_i}{2} \right)^2}_{\text{breaks U(1)}^N\text{ spontaneously}} + \underbrace{\left[\sum_{i=1}^{N-1} \epsilon_i \Phi_i \Phi_{i+1}^3 + \text{h.c.} \right]}_{\text{U(1)}^{N-1}\text{ explicitly broken to discrete sym.}}$$

  $\Longrightarrow$ $(N-1)$ heavy axions + massless QCD axion

  $\hookrightarrow$ DWs

  $\hookrightarrow$ anomalous $\Longrightarrow V_b \sim \Lambda_{\text{QCD}}^4$

- effective decay constant for QCD axion: $f_{\text{eff}} \sim \sqrt{N}\, 3^N f \gg f$

- annihilation: $\sigma \sim m_a f_a^2,\ V_b \sim \Lambda_{\text{QCD}}^4$ $\Longrightarrow$ $T_{\text{ann}} \sim 1\,\text{GeV} \left(\frac{10^7\,\text{GeV}}{f_a} \right)^4 \sqrt{\frac{10\,\text{GeV}}{m_a}}$

Aligned Axion

[Higaki et al. (JHEP 2016)]

- N axions: $$V = \underbrace{\sum_{i=1}^{N} \lambda_i \left(\Phi_i^\dagger \Phi_i - \frac{f_i}{2} \right)^2}_{\text{breaks } \mathrm{U}(1)^N \text{ spontaneously}} + \underbrace{\left[\sum_{i=1}^{N-1} \epsilon_i \Phi_i \Phi_{i+1}^3 + \text{h.c.} \right]}_{\mathrm{U}(1)^{N-1} \text{ explicitly broken to discrete sym.}}$$

$\Longrightarrow$ $(N-1)$ heavy axions + massless QCD axion

$\hookrightarrow$ DWs

$\hookrightarrow$ anomalous $\Longrightarrow V_b \sim \Lambda_{\text{QCD}}^4$

- effective decay constant for QCD axion: $f_{\text{eff}} \sim \sqrt{N}\, 3^N f \gg f$

- annihilation: $\sigma \sim m_a f_a^2,\ V_b \sim \Lambda_{\text{QCD}}^4 \quad \Longrightarrow \quad T_{\text{ann}} \sim 1\,\text{GeV} \left(\frac{10^7\,\text{GeV}}{f_a} \right)^4 \sqrt{\frac{10\,\text{GeV}}{m_a}}$

- heavy axion decay to SM: $\Gamma_{a \to gg} \sim 10^{11}\,\text{s}^{-1} \left(\frac{m_a}{10\,\text{GeV}} \right)^3 \left(\frac{10^7\,\text{GeV}}{f_a} \right)^2$

$\Longrightarrow$ decay before BBN, no N_{eff} constraints

PTA Fit – Aligned Axion DWs

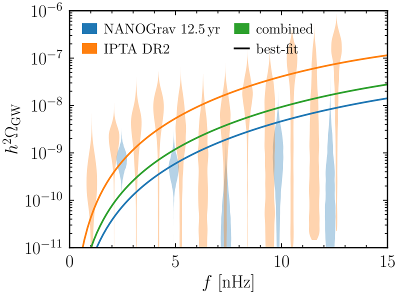

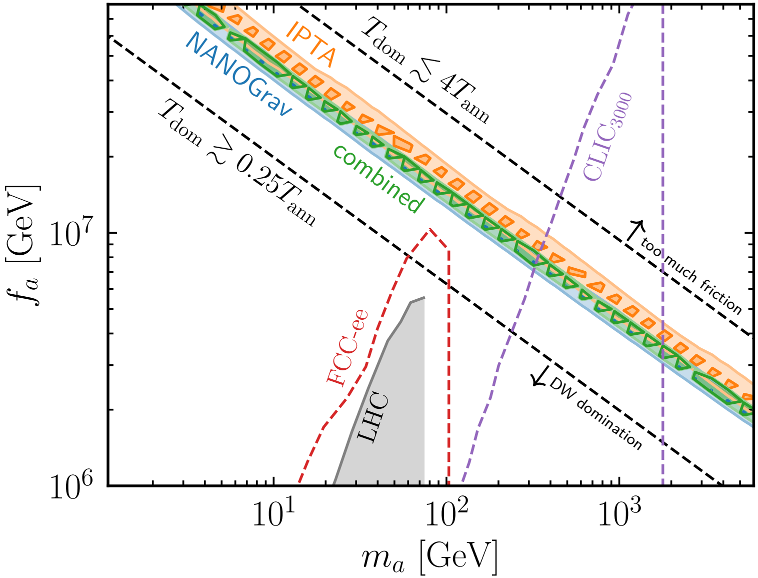

PTA Fit – Aligned Axion DWs

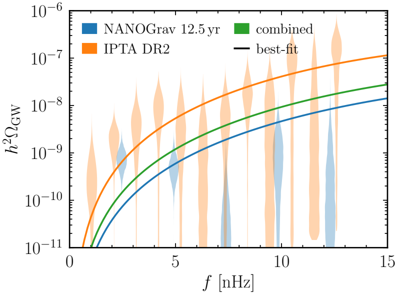

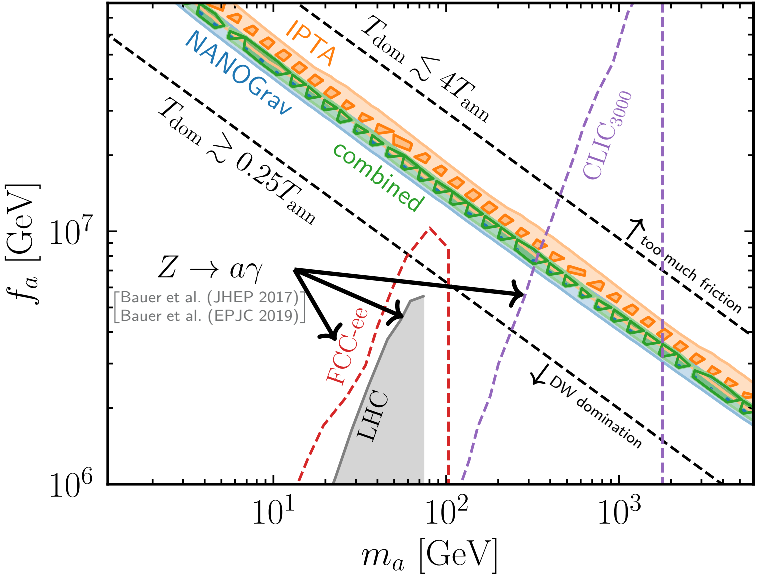

Primordial Black Hole Production

DWs can collapse to PBHs if

$$R < r_S = 2GM$$

$$\sim 2G\left(\frac{4\pi^2}{3}R^3 V_b + 4\pi R^2 \sigma\right)$$

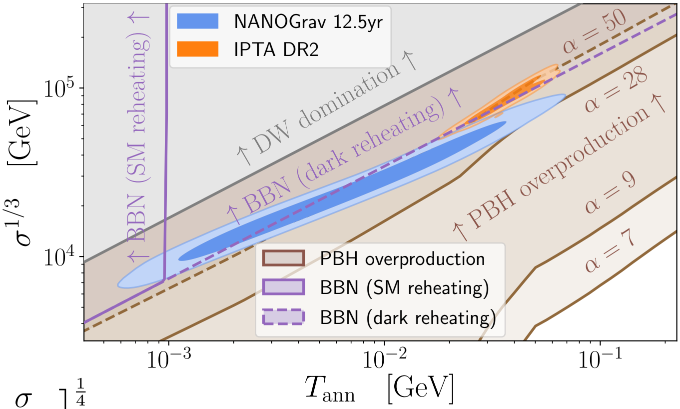

[Gouttenoire, Vitagliano, arXiv:2306.17841 [gr-qc]]

$$\Longrightarrow \quad T_{\mathrm{PBH}} \sim 100\,\mathrm{MeV}\sqrt{\frac{T_{\mathrm{ann}}}{10\,\mathrm{MeV}}}\left[\frac{\sigma}{\mathrm{TeV}^2}\right]^{\frac{1}{4}}$$

Bosonic Instabilities

Misaligment Mechanism

$$\mathcal{L} \supset \frac{1}{2}\partial_\mu\phi\partial^\mu\phi - V(\phi)$$

$$\implies \qquad \ddot{\phi} + 3H\dot{\phi} + m_a^2\phi = 0$$

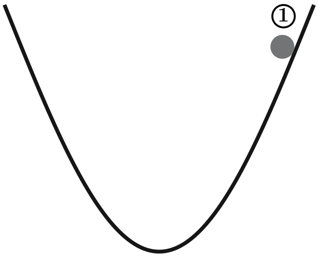

1. $H \gg m_a$: axion pinned by Hubble friction.

Misaligment Mechanism

$$\mathcal{L} \supset \frac{1}{2}\partial_\mu \phi \partial^\mu \phi - V(\phi)$$

$$\Longrightarrow \qquad \ddot{\phi} + 3H\dot{\phi} + m_a^2 \phi = 0$$

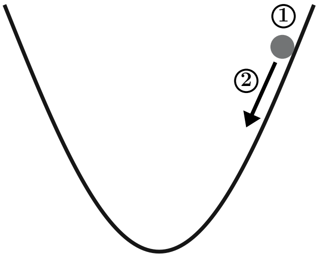

1. $H \gg m_a$: axion pinned by Hubble friction.
2. $H \sim m_a$: axion starts to roll

Misaligment Mechanism

$$\mathcal{L} \supset \frac{1}{2}\partial_\mu\phi\partial^\mu\phi - V(\phi)$$

$$\Longrightarrow \qquad \ddot{\phi} + 3H\dot{\phi} + m_a^2\phi = 0$$

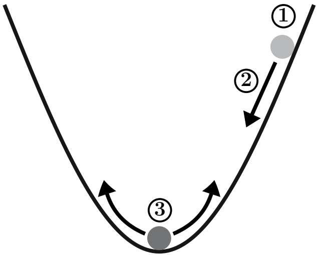

1. $H \gg m_a$: axion pinned by Hubble friction.
2. $H \sim m_a$: axion starts to roll
3. $H \ll m_a$: axion oscillates

Misaligment Mechanism $+$ coupling to dark photon

$$\mathcal{L} \supset \frac{1}{2}\partial_\mu\phi\partial^\mu\phi - V(\phi) - \frac{1}{4}X_{\mu\nu}X^{\mu\nu} - \frac{\alpha}{4}\frac{\phi}{f_a}X_{\mu\nu}\tilde{X}^{\mu\nu}$$

$$\Longrightarrow \qquad \ddot{\phi} + 3H\dot{\phi} + m_a^2\phi = -\frac{\alpha}{f_a}\langle X_{\mu\nu}\tilde{X}^{\mu\nu}\rangle$$

e.g. to deplete axion abundance
Agrawal, Marques-Tavares, Xue (JHEP, 2018)
Kitajima, Sekiguchi, Takahashi (PLB 2018)
or for dark-photon dark-matter
Dror, Harigaya, Narayan (PRD 2019);
Co, Pierce, Zhang, Zhao (PRD 2019);
Bastero-Gil, Santiago, Ubaldi, Vega-Morales (JCAP 2019); Agrawal, Kitajima, Reece, Sekiguchi, Takahashi (PLB 2019)

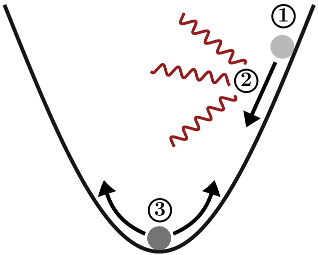

1. $H \gg m_a$: axion pinned by Hubble friction.
2. $H \sim m_a$: axion starts to roll
3. $H \ll m_a$: axion oscillates

$\Longrightarrow$ dark photon production during phase 2 (and 3)

Bosonic Instabilities: Audible Axions

[Machado, Ratzinger, Schwaller, Stefanek (JHEP 2019, PRD 2020)
Ratzinger, Schwaller, Stefanek (SciPost Phys. 2021)]

Misaligment Mechanism + coupling to dark photon

$$\mathcal{L} \supset \frac{1}{2}\partial_\mu\phi\partial^\mu\phi - V(\phi) - \frac{1}{4}X_{\mu\nu}X^{\mu\nu} - \frac{\alpha}{4}\frac{\phi}{f_a}X_{\mu\nu}\tilde{X}^{\mu\nu}$$

$$\Longrightarrow \quad \ddot{\phi} + 3H\dot{\phi} + m_a^2\phi = -\frac{\alpha}{f_a}\langle X_{\mu\nu}\tilde{X}^{\mu\nu}\rangle$$

e.g. to deplete axion abundance
Agrawal, Marques-Tavares, Xue (JHEP, 2018)
Kitajima, Sekiguchi, Takahashi (PLB 2018)
or for dark-photon dark-matter
Dror, Harigaya, Narayan (PRD 2019);
Co, Pierce, Zhang, Zhao (PRD 2019);
Bastero-Gil, Santiago, Ubaldi, Vega-Morales (JCAP 2019); Agrawal, Kitajima, Reece, Sekiguchi, Takahashi (PLB 2019)

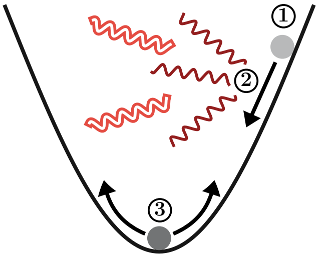

1. $H \gg m_a$: axion pinned by Hubble friction.
2. $H \sim m_a$: axion starts to roll
3. $H \ll m_a$: axion oscillates

$\Longrightarrow$ dark photon production during phase 2 (and 3)

$\Longrightarrow$ gravitational wave emission from dark photons

Dark photon production

dark photon EoM: $$X''_\pm(\tau,k) + \omega^2_\pm(k) X_\pm(\tau,k) = 0 \qquad \omega^2_\pm(k) = \left(k^2 \mp k\frac{\alpha\phi'(\tau)}{f_a}\right)$$

- modes with $k < \left|\frac{\alpha\phi'(\tau)}{f_a}\right|$ experience tachyonic instability in one helicity

Dark photon production

dark photon EoM: $X''_\pm(\tau,k) + \omega^2_\pm(k) X_\pm(\tau,k) = 0$ $\quad \omega^2_\pm(k) = \left(k^2 \mp k\frac{\alpha\phi'(\tau)}{f_a}\right)$

- modes with $k < \left|\frac{\alpha\phi'(\tau)}{f_a}\right|$ experience tachyonic instability in one helicity
- largest growth for $\tilde{k} = \left|\frac{\alpha\phi'(\tau)}{2\,f_a}\right|$ with $\left|\omega^2(\tilde{k})\right| = \tilde{k}^2$

Dark photon production

dark photon EoM: $$X''_{\pm}(\tau,k) + \omega^2_{\pm}(k) X_{\pm}(\tau,k) = 0 \qquad \omega^2_{\pm}(k) = \left(k^2 \mp k\frac{\alpha\phi'(\tau)}{f_a}\right)$$

- modes with $k < \left|\frac{\alpha\phi'(\tau)}{f_a}\right|$ experience tachyonic instability in one helicity
- largest growth for $\tilde{k} = \left|\frac{\alpha\phi'(\tau)}{2\,f_a}\right|$ with $\left|\omega^2(\tilde{k})\right| = \tilde{k}^2$
- for oscillating axion: $\tilde{k} \sim a^{-1/2}$

Dark photon production

dark photon EoM: $$X''_{\pm}(\tau,k) + \omega^2_{\pm}(k) X_{\pm}(\tau,k) = 0 \qquad \omega^2_{\pm}(k) = \left(k^2 \mp k\frac{\alpha\phi'(\tau)}{f_a}\right)$$

- modes with $k < \left|\frac{\alpha\phi'(\tau)}{f_a}\right|$ experience tachyonic instability in one helicity
- largest growth for $\tilde{k} = \left|\frac{\alpha\phi'(\tau)}{2\,f_a}\right|$ with $\left|\omega^2(\tilde{k})\right| = \tilde{k}^2$
- for oscillating axion: $\tilde{k} \sim a^{-1/2}$
- tachyonic band closes when $|\omega(\tilde{k})| < a\, m_a$

  $\Longrightarrow \sim$ energy transfer stops

Dark photon production

dark photon EoM: $X''_\pm(\tau,k) + \omega_\pm^2(k) X_\pm(\tau,k) = 0$ $\quad \omega_\pm^2(k) = \left(k^2 \mp k\frac{\alpha\phi'(\tau)}{f_a}\right)$

- modes with $k < \left|\frac{\alpha\phi'(\tau)}{f_a}\right|$ experience tachyonic instability in one helicity
- largest growth for $\tilde{k} = \left|\frac{\alpha\phi'(\tau)}{2\,f_a}\right|$ with $\left|\omega^2(\tilde{k})\right| = \tilde{k}^2$
- for oscillating axion: $\tilde{k} \sim a^{-1/2}$
- tachyonic band closes when $|\omega(\tilde{k})| < a\, m_a$

$\Longrightarrow$ $\sim$ energy transfer stops

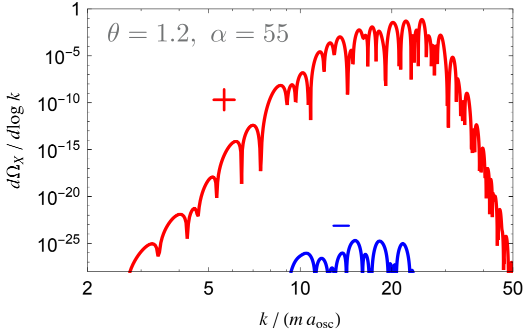

[Machado, Ratzinger, Schwaller, Stefanek (JHEP 2019)]

dark photon spectrum:

- peaked around $\tilde{k} \approx a_{\rm osc} m_a (\alpha\theta/2)^{2/3}$
- first tachyonic helicity dominates

Gravitational Wave Spectrum

GWs generated at t_* around the time when the tachyonic band closes:

- peak frequency:

$$f_{\mathsf{peak}} \sim 2\,\frac{\tilde{k}_*}{a_0} \sim 4\,\mathsf{nHz}\left(\frac{\alpha\,\theta}{100}\right)^{\frac{2}{3}}\left(\frac{m_a}{10^{-15}\,\mathsf{eV}}\right)^{\frac{1}{2}}$$

Gravitational Wave Spectrum

GWs generated at t_* around the time when the tachyonic band closes:

- peak frequency:

$$f_{\text{peak}} \sim 2\,\frac{\tilde{k}_*}{a_0} \sim 4\,\text{nHz}\left(\frac{\alpha\,\theta}{100}\right)^{\frac{2}{3}}\left(\frac{m_a}{10^{-15}\,\text{eV}}\right)^{\frac{1}{2}}$$

- peak amplitude:

$$\Omega_{\text{GW}}^{\text{peak}} \sim \frac{\left(\rho_X^*/f_{\text{peak}}^*\right)^2}{\rho_c\;M_{\text{pl}}^2}\left(\frac{a_*}{a_0}\right)^4 \sim 10^{-7}\left(\frac{f_a}{M_{\text{pl}}}\right)^4\left(100\,\frac{\theta^2}{\alpha}\right)^{\frac{4}{3}}$$

Gravitational Wave Spectrum

GWs generated at t_* around the time when the tachyonic band closes:

- peak frequency:

$$f_{\text{peak}} \sim 2\,\frac{\tilde{k}_*}{a_0} \sim 4\,\text{nHz}\left(\frac{\alpha\,\theta}{100}\right)^{\frac{2}{3}}\left(\frac{m_a}{10^{-15}\,\text{eV}}\right)^{\frac{1}{2}}$$

- peak amplitude:

$$\Omega_{\text{GW}}^{\text{peak}} \sim \frac{\left(\rho_X^*/f_{\text{peak}}^*\right)^2}{\rho_c\ M_{\text{pl}}^2}\left(\frac{a_*}{a_0}\right)^4 \sim 10^{-7}\left(\frac{f_a}{M_{\text{pl}}}\right)^4\left(100\,\frac{\theta^2}{\alpha}\right)^{\frac{4}{3}}$$

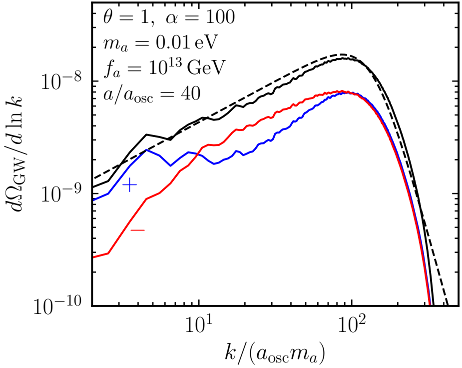

- spectral shape from lattice: [Ratzinger, Schwaller, Stefanek (SciPost Phys. 2022)]

$$\Omega_{\text{GW}} = \Omega_{\text{GW}}^{\text{peak}}\,\mathcal{S}(f/f_{\text{peak}}), \qquad \mathcal{S}(x) = x^{0.73}\left[\frac{1}{2}\left(1+x^{4.2}\right)\right]^{\frac{-4.96-0.73}{4.2}}$$

PTA Fit – Audible Axions

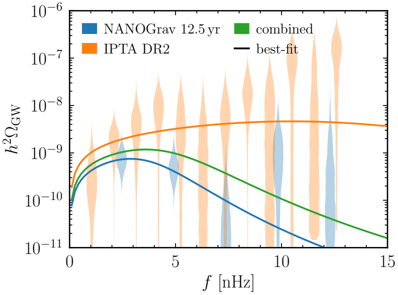

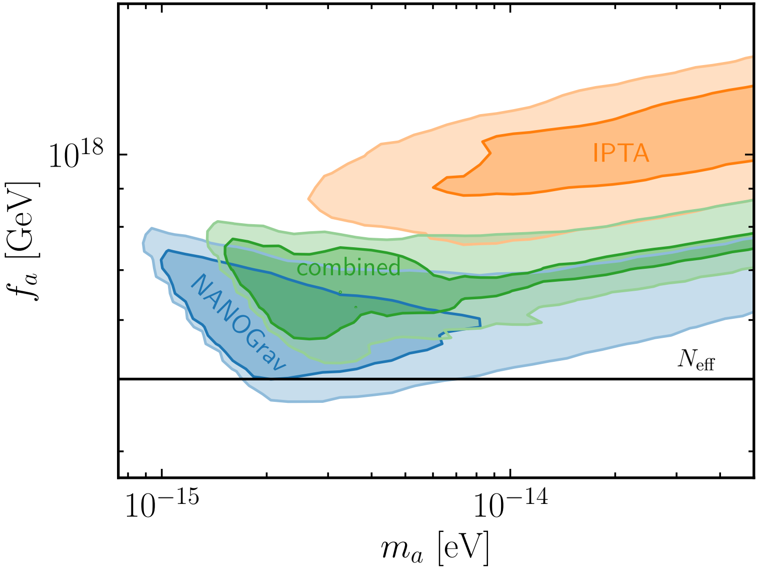

PTA Fit – Audible Axions

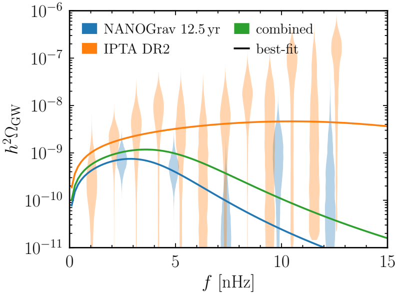

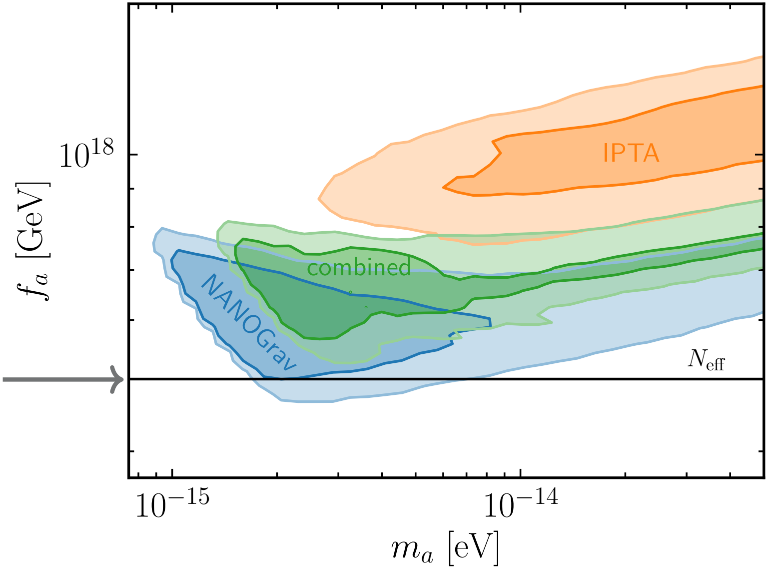

$$\Delta N_{\rm eff} \sim 9.1 \left(\frac{\theta f_a}{M_{\rm pl}}\right)^2$$

(also: $\Omega_a > \Omega_{\rm DM}$)

Conclusions

Fits to NANOGrav 15-year dataset

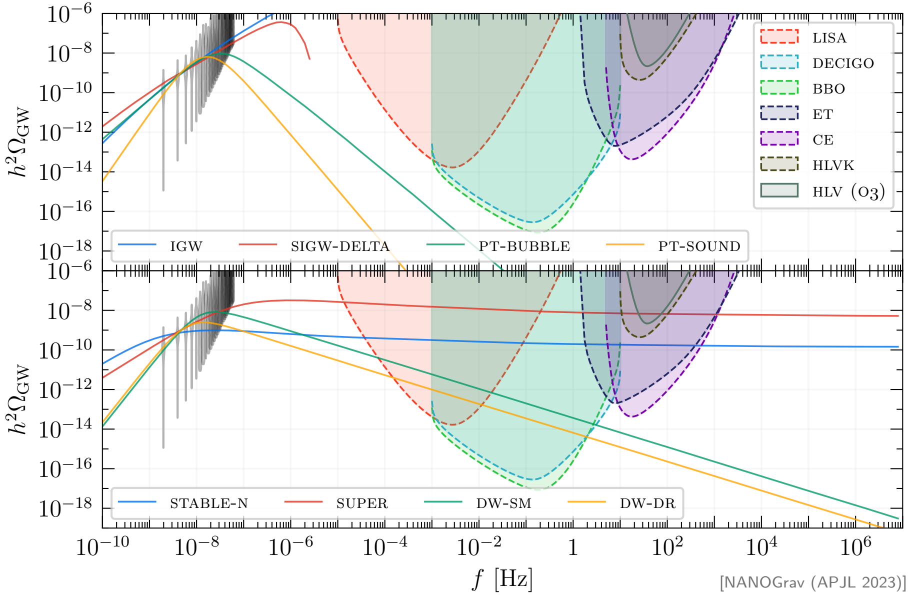

[NANOGrav (APJL 2023)]

Conclusion

Cosmological sources of a SGWB in PTA data:

- phase transition: Coleman-Weinberg model ✔ (at least for 12.5-year dataset)

Conclusion

Cosmological sources of a SGWB in PTA data:

- phase transition: Coleman-Weinberg model ✔ (at least for 12.5-year dataset)
- domain walls: ALP or aligned axion ✘ (PBH overproduction)

Conclusion

Cosmological sources of a SGWB in PTA data:

◌ phase transition:	Coleman-Weinberg model	✔	(at least for 12.5-year dataset)
◌ domain walls:	ALP or aligned axion	✘	(PBH overproduction)
◌ bosonic inst.:	audible axion	✘	(ΔN_{eff}, except for tiny region)

Conclusion

Cosmological sources of a SGWB in PTA data:

phase transition:	Coleman-Weinberg model	✔	(at least for 12.5-year dataset)
domain walls:	ALP or aligned axion	✘	(PBH overproduction)
bosonic inst.:	audible axion	✘	(ΔN_{eff}, except for tiny region)
cosmic strings:	global ALP strings	✘	(ΔN_{eff})
scalar-induced:	single-field w/ inflection point	✘	(CMB)

Conclusion

Cosmological sources of a SGWB in PTA data:

- phase transition: Coleman-Weinberg model ✔ (at least for 12.5-year dataset)
- domain walls: ALP or aligned axion ✘ (PBH overproduction)
- bosonic inst.: audible axion ✘ (ΔN_{eff}, except for tiny region)
- cosmic strings: global ALP strings ✘ (ΔN_{eff})
- scalar-induced: single-field w/ inflection point ✘ (CMB)

Thank you for your attention!

WEIZMANN INSTITUTE OF SCIENCE

Primordial Gravitational Waves and Pulsar Timing Array Data

E.M., Morgante, Puchades Ibáñez, Ramberg, Ratzinger, Schenk, and Schwaller

JHEP **10** (2023), 171 [arXiv:2306.14856 [hep-ph]]

backup slides

PTA Fit – Global ALP Strings

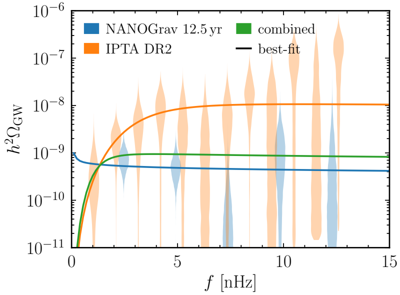

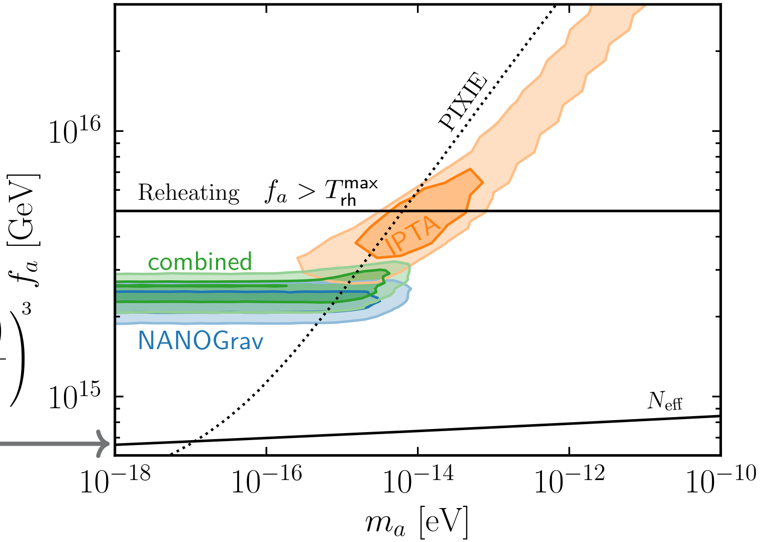

$$\Delta N_{\rm eff} = 0.4 \left(\frac{f_a}{10^{15}\ \mathrm{GeV}}\right)^2 \left(\frac{\log\left(\frac{f_a}{m_a}\right)}{80}\right)^3$$

PTA Fit – Scalar-Induced GWs

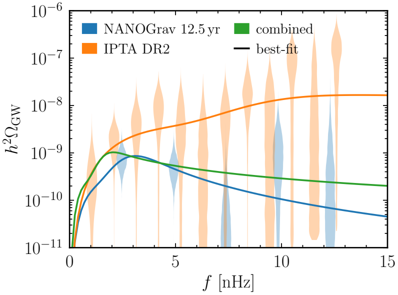

$$P_\zeta(k) = \begin{cases} \dfrac{A_\zeta\, e^{-\frac{\log^2(k/k_*)}{2\,\Delta^2}}}{\sqrt{2\pi}\,\Delta}, & \dfrac{k}{k_*} < e^{n\Delta^2} \\ \dfrac{A_\zeta\, e^{n\Delta^2}}{\sqrt{2\pi}\,\Delta}\left(\dfrac{k}{k_*}\right)^{-n}, & \dfrac{k}{k_*} > e^{n\Delta^2} \end{cases}$$

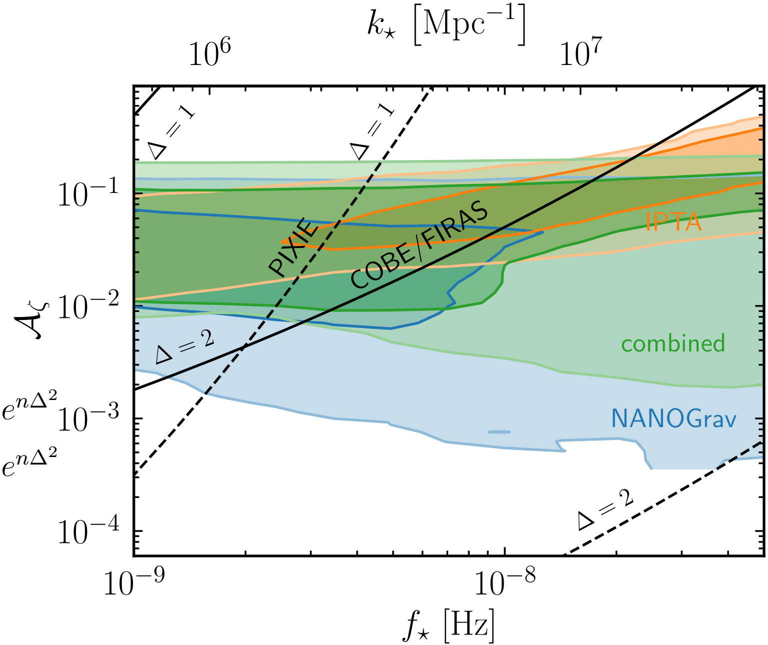

Triangle Plots I

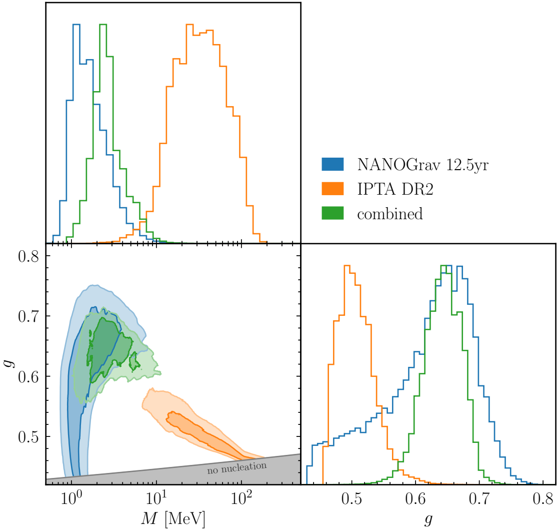

PhT in Coleman-Weinberg model

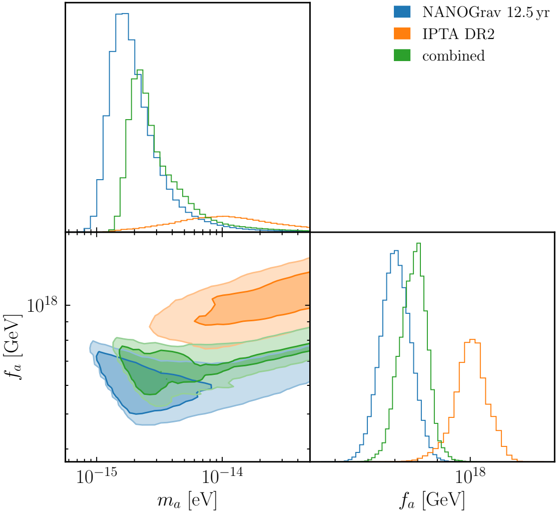

audible axions

Triangle Plots II

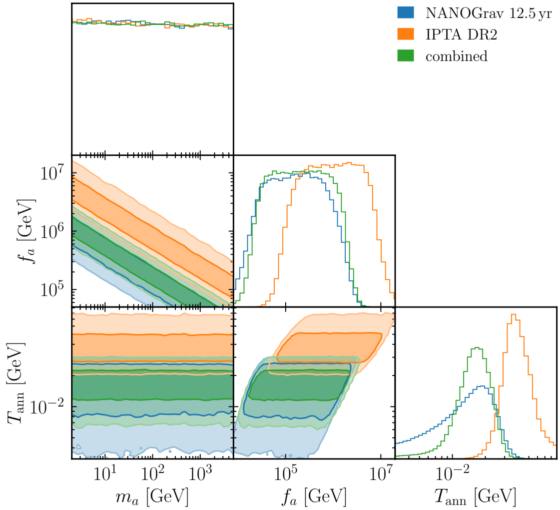

ALP domain walls

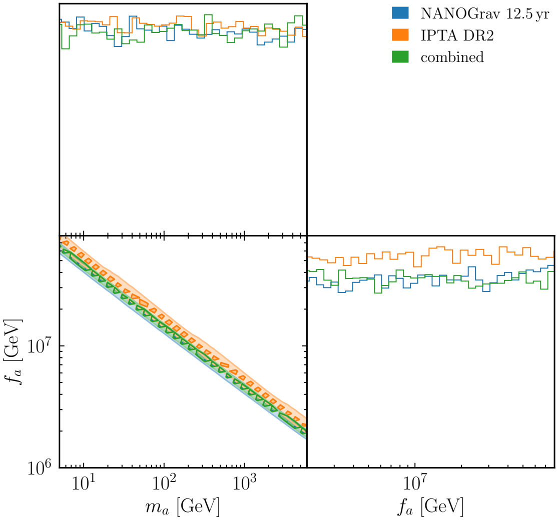

aligned axion domain walls

Triangle Plots III

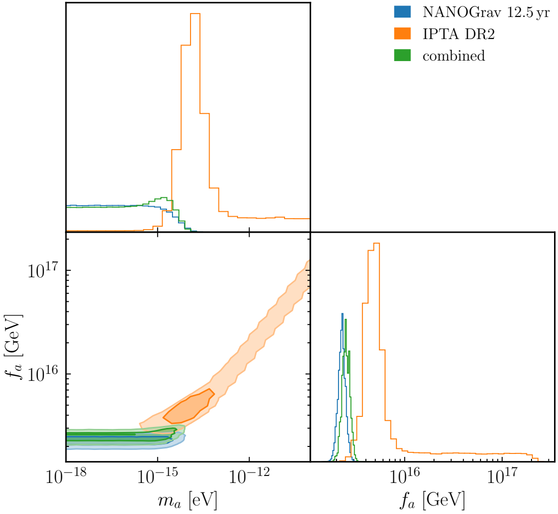

global ALP strings

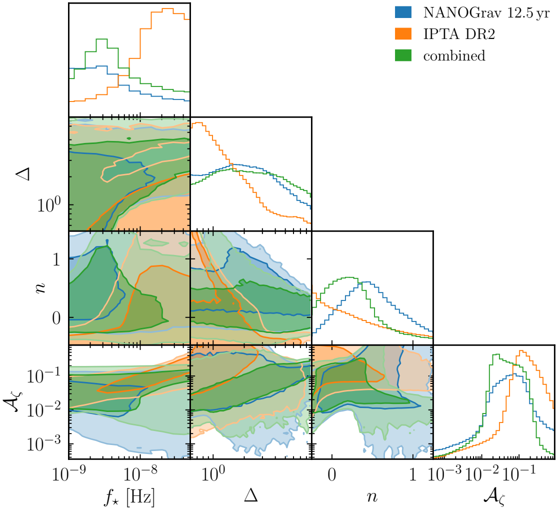

scalar-induced GWs

Single-field Inflation with Inflection Point

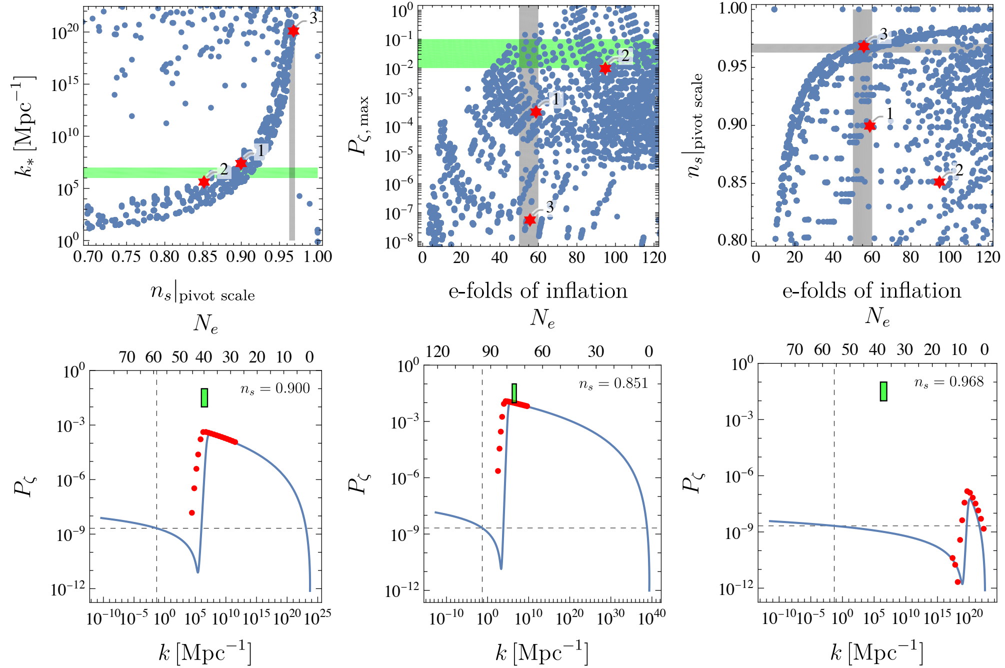

NANOGrav 15-year dataset: Bayesian Evidence

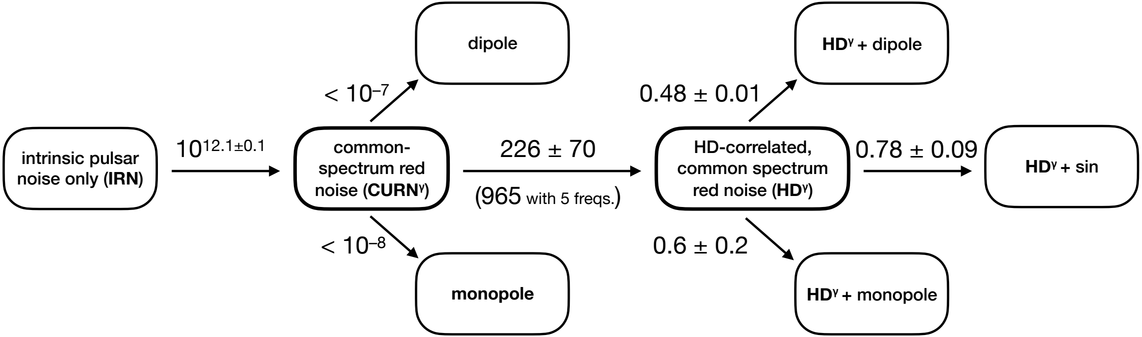

[NANOGrav (APJL 2023)]

NANOGrav 15-year dataset: Bayes Factors

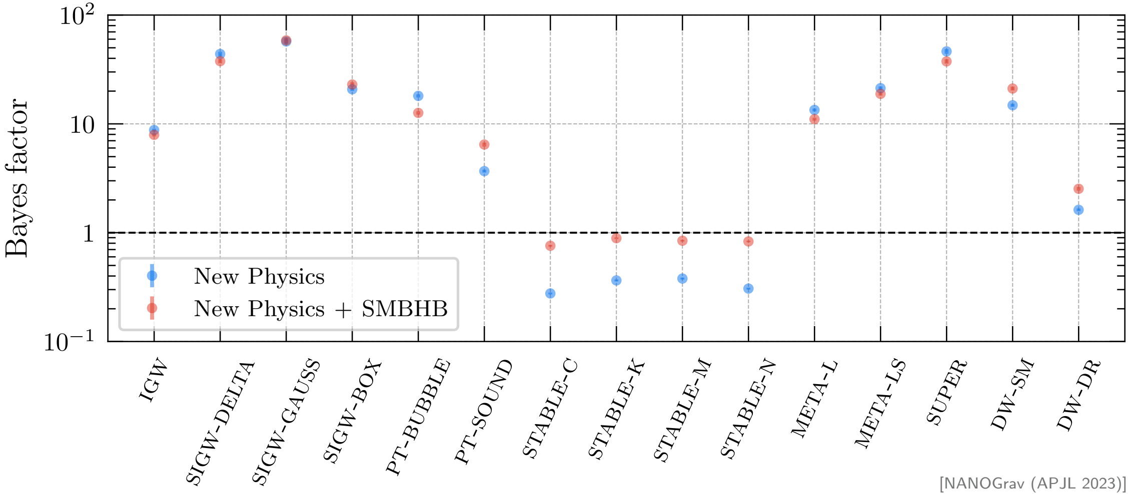

[NANOGrav (APJL 2023)]